4

Evaluation of the Frequency Response of AC Transmission Based Offshore Wind Farms

M. Zubiaga[1], G. Abad[1], J. A. Barrena[1], S. Aurtenetxea[2] and A. Cárcar[2]
[1]*University of Mondragon,*
[2]*Ingeteam Corporation*
Spain

1. Introduction

Nowadays, the state of the distribution grids is significantly different in comparison with the state of two decades ago. One important reason for that is the existence of non-lineal loads. These non-lineal loads can provoke disturbances, like a high level harmonics in current and voltages (Pigazo, 2004).
In the same way, there is consolidating a distributed generation system for the distribution grids. This kind of grids contain a combination of many types of generation plants, like cogeneration, combined cycle, wind farms, photovoltaic…Thus, if the distribution grid is made up with many small and medium generation plants, the waveform of the voltage may be distorted.
In conclusion, the electric transmission and distribution system is evolving to a scenario with multiple harmonic sources. So, the frequency analysis of the electric grids is becoming an important tool, because can help to improve their efficiency reducing the power associated to these disturbances.
As regards to AC offshore wind farms, the interaction between the offshore installations and the onshore grid can cause harmonic amplifications. This aspect is not trivial, because as a result of this harmonic amplification, the harmonic level in the point of common coupling of the wind farm can be unacceptable for the grid code requirements.
Offshore wind farms are connected through a widespread medium voltage submarine cable network and connected to the transmission system by long high voltage cables. Submarine power cables, unlike underground land cables need to be heavily armored and are consequently complicated structures. So, in particular this type of power cables have a relatively larger shunt capacitance compared to overhead lines which make them able to participate more in resonant scenarios (Kocewiak et al., 2010).
The present chapter evaluates the frequency behavior of the offshore wind farms at normal operation (steady state), in function of design procedure parameters like: the cable length / characteristics, transformers connection and leakage inductance or inter-turbine grids configuration. The analysis is performed from the point of view of the wind turbines, considering them as potential harmonic sources. Thus, the knowledge of the frequency behavior of the offshore wind farm can help to avoid as much a possible the harmonic amplification, at the design stage of the wind farm. This presents new challenges in relation to understanding the nature, propagation and effects of the harmonics.

2. Power transmission lines

2.1 Power transmission cables

The purpose of a power cable is to carry electricity safely from the power source to different loads. In order to accomplish this goal, the cable is made up with some components or parts. Fig. 1 shows a description of the cable's components, which are:

Conductor

The conductor is referred to the part or parts of the cable which carry the electric power. Electric cables can be made up by one conductor (mono-phase cables), three (three-phase cables), four, etc.

Insulation

Dielectric material layer with the purpose of provide insulation between conductors of different phases or between phases and ground.

Shield

metal coating, which covers the entire length of the cable. It is used to confine the electric field inside the cable and distribute uniformly this field.

Armor or sheath

Layer of heavy duty material used to protect the components of the cable from the external environment.

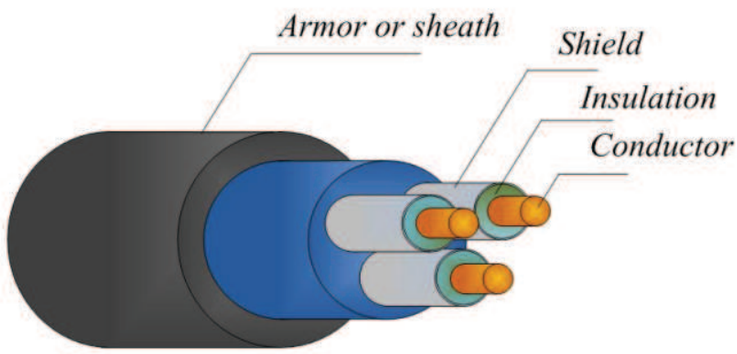

Fig. 1. Generic representation of an electric power cable

The electric behavior of the power transmission cable can be represented by several electromagnetic phenomena, yielding to behavioral characteristics such as; the conductor of the cable presents small resistivity or when an electric current flow through a conductor generates a magnetic field around it. Another effect is caused by the voltage difference from the conductor to ground, which provokes the storage of electric charge in the conductor. Finally, there is a leakage current to ground. The dielectric is a material with low conductivity, but not zero.

Thus, through the years, many authors have agreed that a transmission cable can be represented electrically for each differential length with distributed *RLCG* parameters, (Jiang, 2005; Sánchez, 2003; Weedy & Cory, 1998). Where:

- The distributed resistance *R* of the conductors is represented by a series resistor (expressed in ohms per unit length).

- The distributed inductance *L* (due to the magnetic field around the wires, self-inductance, etc.) is represented by a series inductor (henries per unit length).
- The capacitance *C* between the two conductors is represented by a shunt capacitor *C* (farads per unit length).
- The conductance *G* of the dielectric material separating the two conductors is represented by a conductance *G* shunted between the signal wire and the return wire (Siemens per unit length).

In DC circuits, the current density is similar in all the cross section of the conductor, but in AC circuits, the current density is greater near the outer surface of the conductor. This effect is known as the skin effect.

Due to this phenomenon, AC resistance of the conductor is greater than DC resistance. Near to the center of the conductor there are more lines of magnetic force than near the rim. This causes an increment in the inductance toward the center and the current tends to crowd toward the outer surface. So at higher frequencies the effective cross section area of the conductor decreases and AC resistance increases.

In short, the skin effect causes a variation in the parameters of the cable, due to the non uniform distribution of the current through the cross section of the cable. This variation is in function of the frequency, producing that the *RGLC* parameters are frequency dependent. If this effect is taken into account the electric representation of the cable for each differential length yields as shown in Fig. 2.

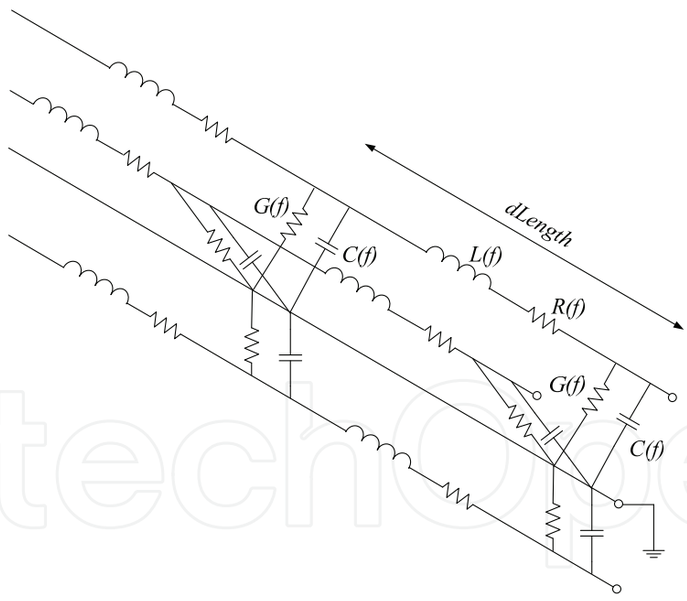

Fig. 2. Electrical representation of the cable per differential length with frequency dependent parameters

2.2 Modeling options of the power transmission cable

Based on the electric representation of the cables and depending on the cable model requirements, it is possible to perform more or less simplifications, in order to maintain the accuracy of the model and reduce its complexity. Thus, there are several ways for modeling a cable; these models can be classified as follows (Restrepo et al., 2008).

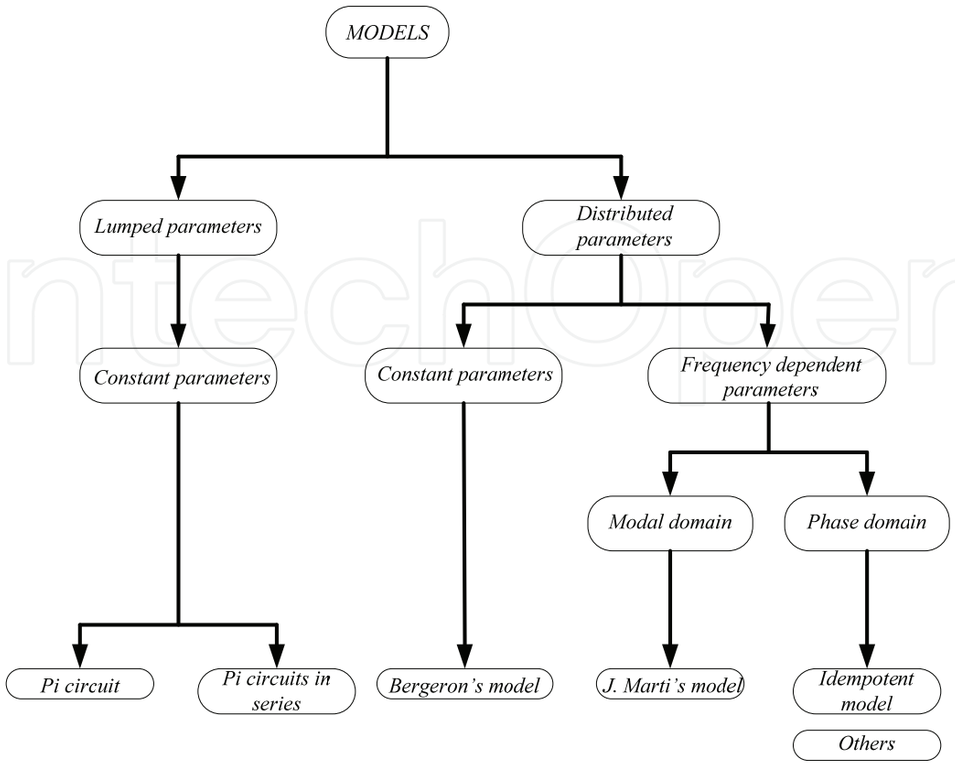

Fig. 3. Classification of the different types of cable models

2.2.1 Frequency dependent model in phase domain (Idempotent model)

The selected model to carry out the evaluation of the frequency response of the offshore wind farm, is the PSCAD's frequency dependent phase model based on the idempotent model. The reason to select the most complex and accurate model is because the cable model has to represent a wide frequency range.

The Idempotent model is analyzed in (Castellanos et al., 1997; Marcano, 1996; Restrepo et al., 2008).

The idempotent model with some changes / improvements detailed in (Gustavsen et al., 1999) is used in PSCAD as the most accurate model. Moreover, the PSCAD user's guide guaranties that its cable model, frequency dependent in phase domain is very accurate (Power System Computer Aided Design [PSCAD], 2003). This model used by PSCAD also has been successfully validated experimentally in (Nian, 2009; Meier, 2009).

2.3 Cable parameter adaptation to PSCAD

Based on the physical characteristics of one specific cable as served in Table 1 (Courtesy of General Cable), PSCAD solves / estimates the equivalent impedances (*RLGC* parameters) for the electric representation of the cable shown in, Fig. 2. In this way, for complex models, where many parameters and detailed electric specifications are required, the definition of the cable is simpler.

PSCAD provides a template to fill into it the data of the cable. Nevertheless, for complex cables it is not possible to represent the whole cable. The template has concentric, circular and homogeneous layers to introduce the data of the cable. Even though there are subsea

cables made up with other physic characteristics like: semiconductor layers, conductors made up with crown of strands or the fill between conductors.
Due to the impossibility to fill in directly the data of the cable to the PSCAD software, the physic parameters have to be modified / corrected. The purpose of this correction is to achieve the same value of the equivalent impedances for PSCAD estimation and the cable manufacturers. The modified parameters are those ones related to the conductor, shield and insulation.

Parameter	Value
Rated voltage	87 / 150*kV*
Rated current	1088*A*
Conductors cross section	1.200mm^2
Separation between conductors	97.839996*mm*
Buried depth	1*m*
Shields cross section	30mm^2
Shield type	Metallic strip
Armor type	Strands crown
Diameter of conductor	43,5*mm*
Insulation thickness	20*mm*
Diameter upon the insulation	88,5*mm*
Diameter down the sheath	215,6*mm*
Diameter down the armor	226,7*mm*
Sheath thickness	8,9*mm*
External diameter	244,5*mm*
Relative dielectric constant	2,50
Resistivity of the conductor d.c. at 20°C	0,0151*Ohm/km*
Resistivity of the conductor a.c.	0,0205*Ohm/km*
Resistivity of the shield d.c. at 20°C	0,6264*Ohm/km*
Rated capacitance of the cable	0,233$\mu F/km$
Inductance of the cable	0,352*mH/km*

Table 1. Cable characteristics provided by General Cable

2.3.1 Conductor

Looking at Table 1, the conductor has a 43.5mm diameter and also an effective cross section of 1200mm². If the conductor is considered as a solid core, homogenous and circular (as the template of PSCAD does), the cross section for this diameter (equation (1)) is not the same.

$$A = \pi \cdot r^2 = \pi \cdot 21.75^2 = 1486.17 mm^2 \quad (1)$$

Therefore, to solve this difference it is necessary to correct the resistivity of the conductor ρ. To this end, at the first step the real resistivity of the conductor is calculated (based on the data of the cable given by the manufacturer), equations (2) -(3).

$$R_{DC} = \frac{\rho_c \cdot l}{A_c} = 0.0151 \ ohm/Km \quad (2)$$

$$\rho_c = \frac{R_{DC} \cdot A_c}{l} = 1.812 \cdot 10^{-8} \tag{3}$$

Where: ρ_c is the resistivity, l is the length of the cable and A_c is the effective cross section of the conductor (1200 mm²).
At the second step, the resistivity of the conductor's material is modified in order to maintain the same absolute resistance of the conductor, (Nian, 2009). Based on the conductor radius given by the manufacturer, in function of the effective cross section and the real cross section, is corrected the resistivity:

$$\rho_c{}' = \rho_c \frac{\pi \cdot r^2}{A_c} = 2.24412 \cdot 10^{-8} \tag{4}$$

To verify this estimation, the absolute resistance of the conductor at 50 Hz is calculated with equation (5). From this equation, it is possible to achieve practically the same results in comparison with the characteristics of the manufacturer.

$$R_{a.c.}(50) = \frac{\rho_c}{\delta_{50}} \cdot \frac{l}{\pi\left(D - \delta_{50}\right)} = 0.0204 \ \ ohm / Km \tag{5}$$

$$\delta_{50} = \sqrt{\frac{2 \cdot \rho_c}{\omega \cdot \mu}} = 0.010662 \tag{6}$$

Where: l is the length of the cable, D is the diameter of the conductor, ρ_c is the resistivity, ω is the angular speed of the current ($2\pi f$), μ is the absolute magnetic permeability of the conductor ($\mu_0\,\mu_r$), μ_0 is the magnetic constant or the permeability of the free space ($4\pi \times 10^{-7}$ N/A²) and μ_r is the relative magnetic permeability.

2.3.2 Shield

The next parameters that must be modified are the size of the diameter of the insulation and its relative permeability, in order to maintain the shield with 30mm² and the same capacitive component.
Assuming that the outer diameter of the shield's conductor layer is 88.5mm, it is possible to obtain the inner diameter, equations (7) - (9).

$$A_s = R_s^2 - r_s^2 \tag{7}$$

$$30mm2 = 44.45^2 - r_s^2 \tag{8}$$

$$r_s = \sqrt{44.25^2 - 30} = 43.9mm \tag{9}$$

2.3.3 Insulation

To correct the area of the shield the radius of the insulation is modified. As a result, the value of the capacitive component using the radius calculated in equation (9) is slightly different in comparison with the characteristic provided by the manufactures.
Therefore, to represent correctly the submarine cable, the dielectric constant is corrected in order to represent in PSCAD the same the capacitive component of the manufacturer's data sheet, equations (10) - (11).

$$\varepsilon_r = 0.233 \cdot 17.97 \cdot \ln\left(43.9/21.75\right) = 2.94 \tag{10}$$

$$C = \frac{\varepsilon_r}{17.97 \cdot \ln\left(b/a\right)} = \frac{2.94}{17.97 \cdot \ln\left(43.9/21.75\right)} = 0.233 \quad \mu F / Km \tag{11}$$

2.3.4 Measure with PSCAD the adapted parameters

To validate the modification of parameters carried out in the preceding sections, a submarine cable in PSCAD (Fig. 4) is defined, based on the physic data of the cable shown in Table 1 with these modifications. Then, using PSCAD software, its internal *RLCG* parameters are obtained, Table 2.

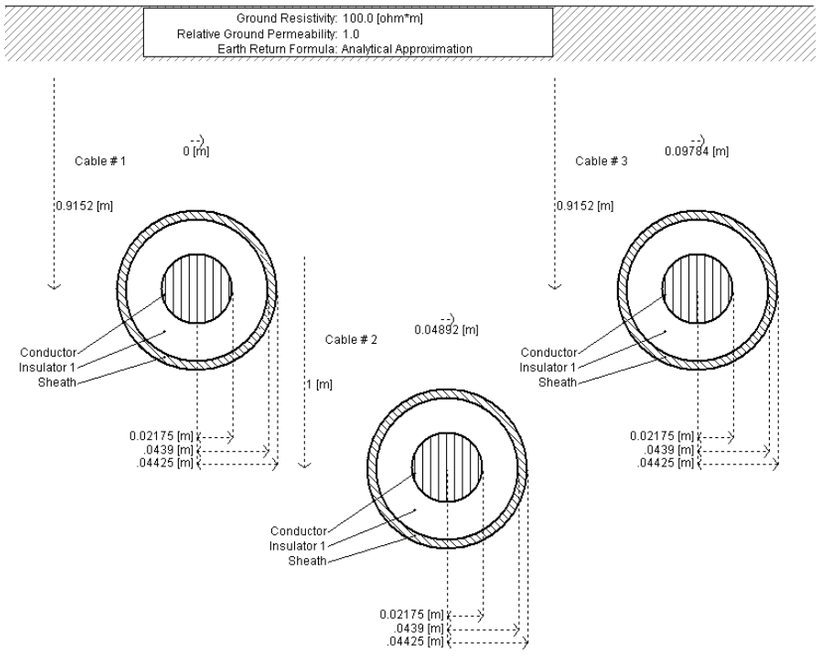

Fig. 4. Graphic representation in PSCAD of the three-phase cable

	Resistivity	Inductivity	Capacitance
Electric parameters (50*Hz*)	0.0311***Ohm/km*	0.334*mH/km*	0.233μ*F/km*

*Resistivity without taking into account the shield, conductor 0.0190*Ohm/km*

Table 2. *RGLC* electrical parameters calculated by PSCAD in function of the physic dimensions and characteristics

From the results displayed in Table 2, it is possible to see that the electrical parameters calculated by PSCAD are substantially similar to the parameters specified by the manufacturer.

3. Frequency response of the transmission system via PSCAD simulation

3.1 Frequency response of the basic transmission system via PSCAD simulation

The transmission system is the part of the offshore wind farm which makes possible the energy transmission from the collector point (offshore) to the point of common coupling (onshore), in other words, the physic medium to transfer the energy from the wind farm to the main grid and all the support devices.

The transmission system is made up by the step-up transformer, the submarine cable, reactive power compensation elements (if required), and the support devices to integrate the energy in the main grid (if required).

The knowledge of the frequency response of the transmission system and the influence of each component upon this frequency response can help to avoid undesired resonances and harmonics. For that purpose, firstly, in this section the simplest lay-out for the transmission system (transformer, cable and grid, Fig. 5) is considered, i.e. the necessary elements to perform the energy transmission, without the support devices to improve the transmission.

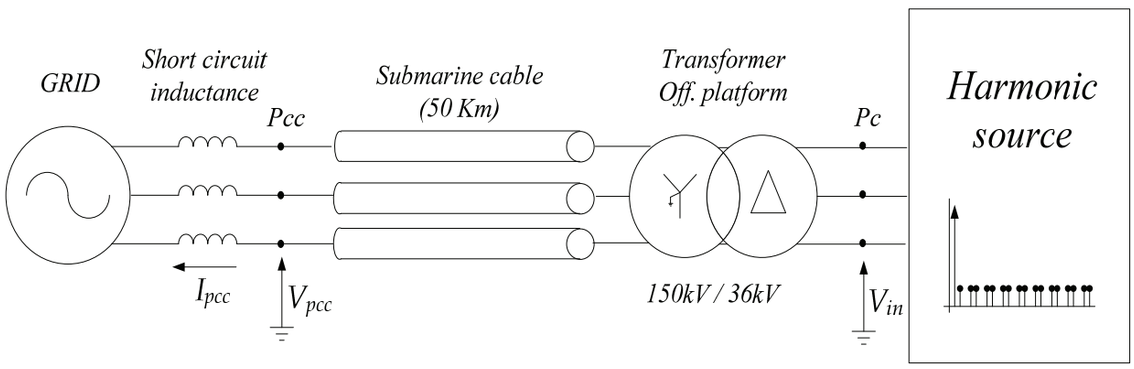

Fig. 5. Simulation scenario of the simplest lay-out of the transmission system: the step-up transformer, the submarine cables and the distribution grid

To calculate the impedance of the transmission system in function of the frequency, a harmonic voltage source is used. The harmonic train of input voltage (V_{in}), is composed by sinusoidal components in the range of frequencies: 50-5000Hz. The amplitude of these harmonic voltages is 10% of the fundamental (50Hz-150kV). Starting from the 50Hz, the harmonic train has voltage components separated 10Hz one from other, as illustrated in Fig. 6. These input harmonics in a simplified way can represent the effect of the harmonics generated by the wind turbines, when they are generating energy from the wind.

Measuring the current at the PCC (I_{pcc}) and performing the FFT (Fast Fourier Transform) of the signal, it is possible to obtain the impedance of the transmission system for each one of the excited frequencies, i.e. it is possible to obtain the evolution of the impedance in function of the frequency.

To model the grid in a simple manner, a voltage source and short circuit impedance is used. Its characteristics are summarized in Table 3. The transformer's connection is Δ- gY, while its characteristics are shown in Table 4. Finally, the cable characteristics and cable model are the same of the section 2.

The frequency response of the described transmission system layout is depicted in Fig. 7.

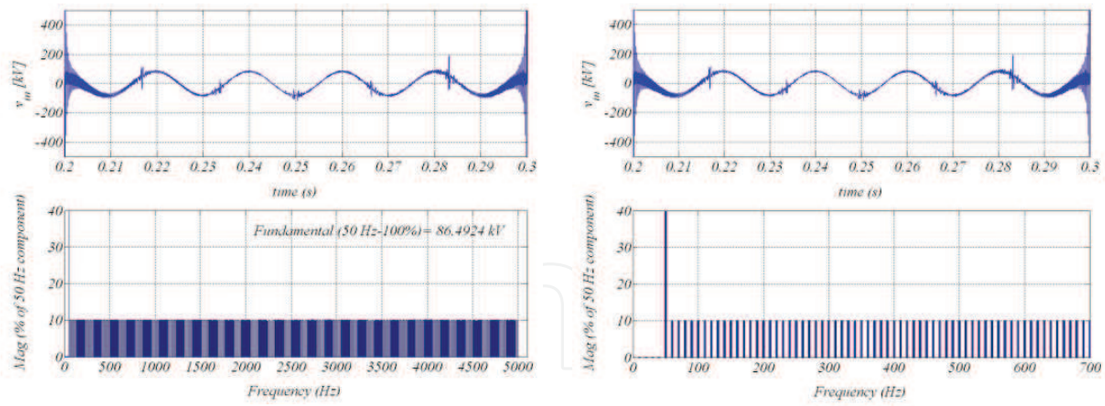

(a) (b)

Fig. 6. Harmonic voltage train applied to the submarine cable model (resolution 10 Hz)

Parameter	Value
Nominal power (Pn)	150*MW*
Nominal voltage (Vn)	150*kV*
Short circuit inductance	5%

Table 3. Characteristics of the main grid

Parameter	Value
Rated power	150*MVA*
Primary voltage	33*kV*
Secondary voltage	150*kV*
Connection	Δ- gY
Transformers leakage resistance	1%
Transformers leakage inductance	6%
No load losses	1,78%

Table 4. Characteristics of the step-up transformer

Looking at Fig. 7, it is possible to observe that all the multiples of the 3rd order harmonics generated in the wind turbines, cannot trespass to the PCC. This occurs because between these points is placed a transformer with star (grounded)-delta connection.

The transmission system is composed with several inductive components, like the transformer or the short circuit impedance of the main grid. This inductive impedances provokes a significant attenuation of the high frequencies, as can be seen in Fig. 7 (c), thus, the high frequency harmonic voltages do not affect to the current of the PCC. In fact, in the present analysis, the harmonics higher than 700Hz almost do not affect to the current at PCC.

However, the interaction of the inductive component of the transmission system with the capacitive component of the submarine cable provokes a resonance at 400Hz, becoming these frequencies which are around the 400Hz potentially problematic.

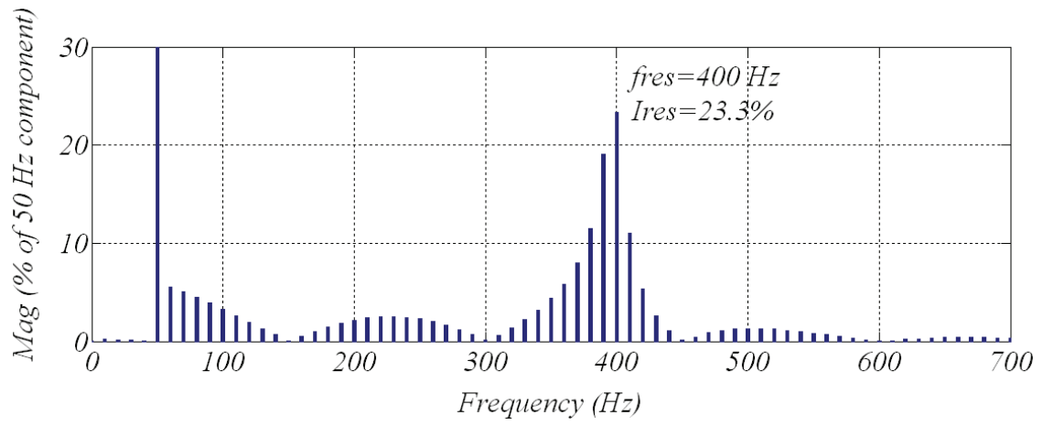

(a)

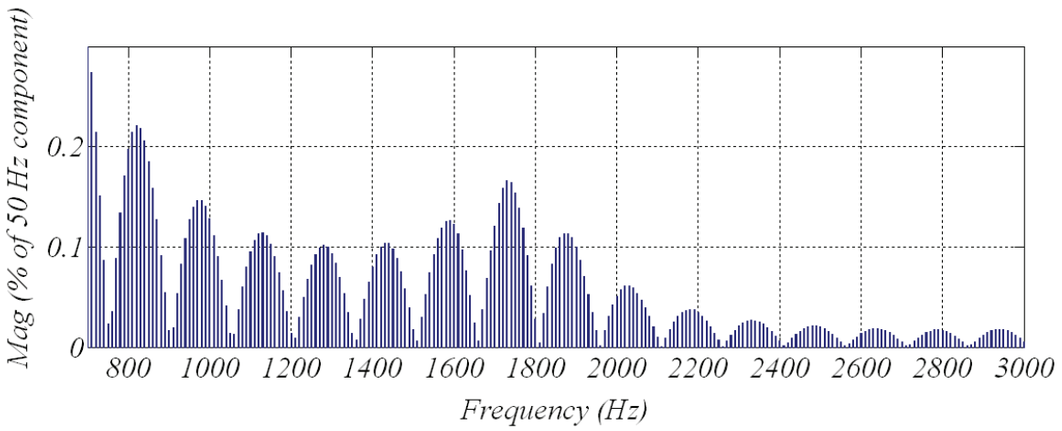

(b)

Fig. 7. Frequency response of the transmission system with only: grid impedance, step-up transformer and submarine cable (50 Km). FFT of the current at PCC: (a) detail in the neighborhood of the main resonance and (b) detail in high frequencies

3.2 The effect of the different parts of the transmission system in its frequency response

The analysis of how affects each one of the elements of the transmission system in its frequency response is the first step to avoid undesired resonances and optimize the transmission system design.

Therefore, this section analyses the frequency response of the transmission system varying the characteristics (impedance) of its three main components:

- The leakage impedance of the step-up transformer.
- The impedance of the submarine transmission line (variation of the cable length).
- The short circuit impedance of the main grid.

Firstly the influence of the step-up transformer is evaluated. Based on the same scenario of the Fig. 5 and applying the same harmonic train (Fig. 6), the frequency responses of the transmission system are obtained. In this first case, the transformer's leakage inductance has a variation from 3% to 12%, the results are depicted in Fig. 8.

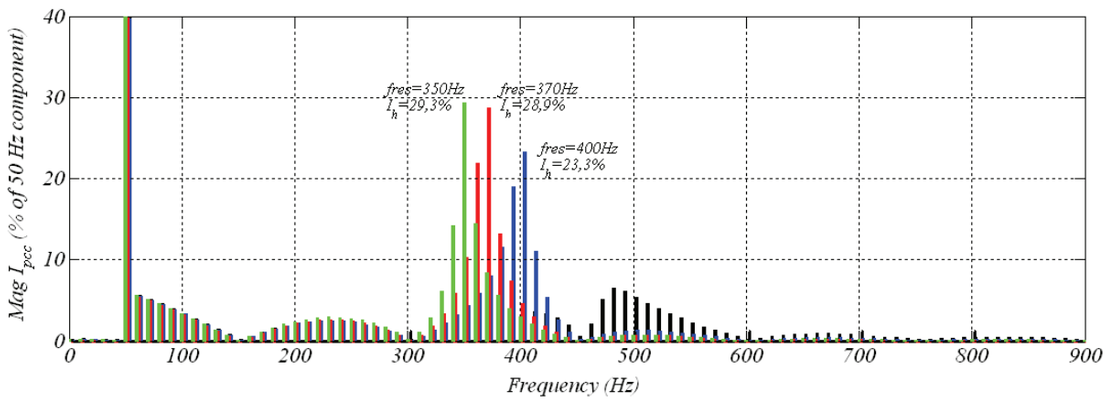

Fig. 8. Frequency response of the transmission system varying the leakage inductance of the step-up transformer from: 3% (black), 6% (blue), 9% (red) and 12% (green)

As is shown in Fig. 8, as the leakage inductance of the step-up transformer increases, the frequency of the resonance decreases (from 450Hz to 350Hz).
For the specific case where the leakage inductance is 3%, it is possible to see how the transformer connection does not allows to cross to the PCC the harmonics close to the resonance, Fig. 9. The resonance is still there (450Hz), but, there are not harmonics to be amplified.

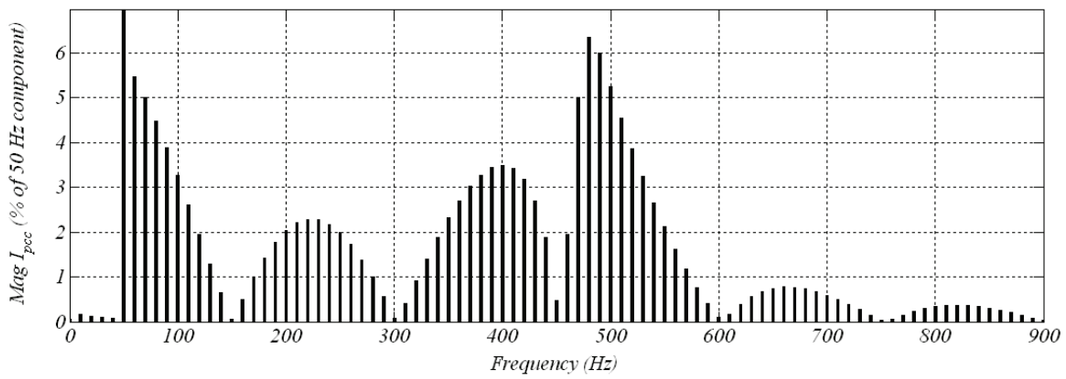

Fig. 9. Frequency response of the transmission system with a leakage inductance of 3% of the step-up transformer

The harmonic train used for this analysis has components into de 50-5000Hz range, but not continuously in all this range, the harmonic source generates harmonic voltages in steps of 10 Hz. Thus, using the harmonic train is possible to determinate the resonance with 10 Hz accuracy, i.e. the system has a 10 Hz accuracy
With regards to the amplitude of the resonance, this varies very quickly in few Hz close to the resonance frequency. As a consequence, if the harmonic resonance matches up with the exact resonance frequency, the measured amplitude in the simulation will be bigger than in cases where the harmonics in the train are close to the exact frequency of the resonance. Thus, this analysis can measure accurately the frequency of the resonance, but not the amplitude, the amplitude is only an approximated value.

In the next step of the analysis, the influence of the cable length in the range of 20Km to 110Km is evaluated. The frequency response of the considered transmission system with this variation is shown in Fig. 10.

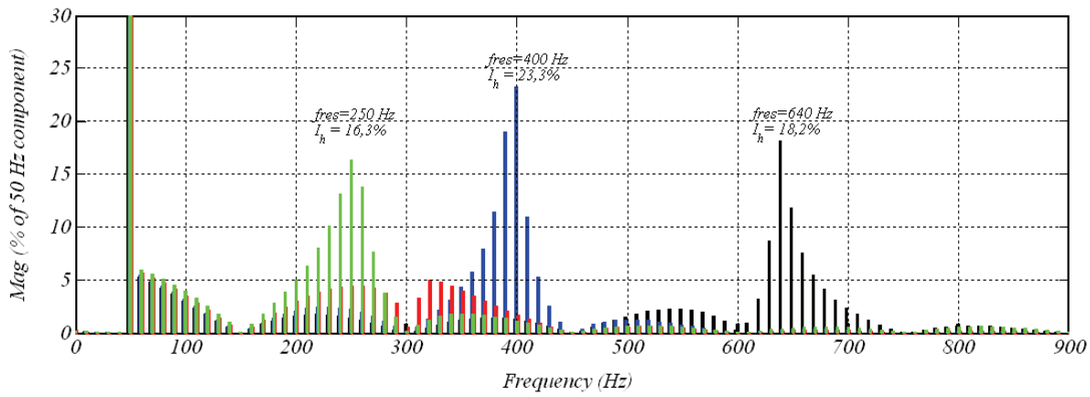

Fig. 10. Frequency response of the transmission system varying the cable length from: 20Km (black), 50Km (blue), 80Km (green) and 110Km (red)

In this case, as the submarine cable length increases, the resonance frequency decreases. Note that the resonance of the transmission system with 80Km cable disappears, because in this case also all the multiples of the 3rd order harmonics cannot trespass the transformer.
In the third and last case there are considered different values for the short circuit impedance. This variation is from the 2 % to 11 %, the simulation results are depicted in Fig. 11

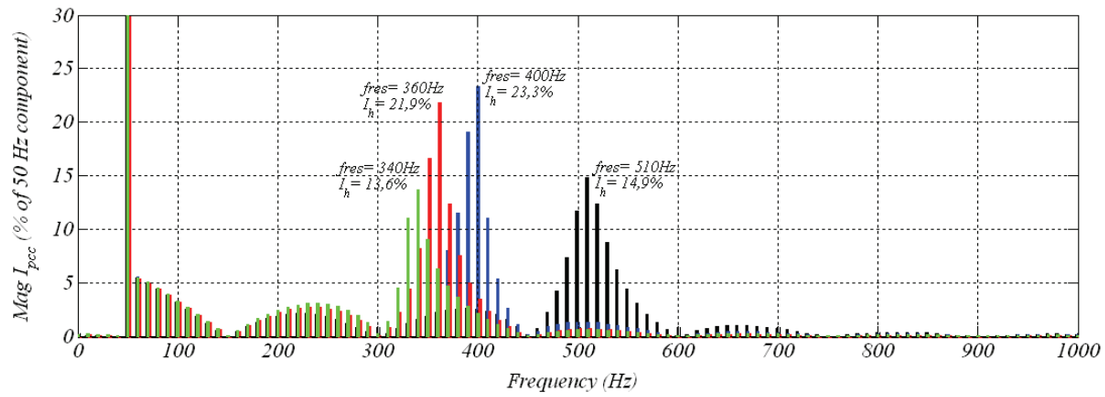

Fig. 11. Frequency response of the transmission system varying the short circuit impedance from: 2 % (black), 5 % (blue), 8 % (green) and 11 % (red)

In this last case, increasing the short circuit impedance decreases the resonance frequency, i.e. as in the two previous cases, increasing the inductive impedance or the capacitive impedance the frequency of the resonance decreases. In the analyzed cases, the biggest variation is between 640Hz-250Hz, caused varying the cable length from 20Km to 110Km. However, in most of the cases the resonance is between 450Hz and 250Hz. In concordance with these results, in (Breuer & Christl, 2006) is highlighted that AC transmission systems in conjunction with step-up transformer of the offshore substation, present the risk to amplify harmonics at low frequencies (inherently 3rd, 5th and 7th order harmonics).

3.3 Frequency response of the transmission system via analytic calculus

The objective of this section is to estimate the main resonance frequency in a simple and accurate way, alternatively to the method described in the previous section. Thus this section studies the calculation of the first resonance frequency of the transmission system, which is the main characteristic of the frequency response, using two different analytic ways.

To characterize in an easy way the main resonance frequency, with a potential risk of harmonic amplification, in (Plotkin et al., 2008) is presented a simple method. This approximation only takes into account the capacitive component of the submarine cable, neglecting the resistive and inductive components. In this way, it is possible to simplify the whole transmission system as an equivalent *RLC* circuit. Then, the resonance frequency of this simplified *RLC* circuit serves to approximate the resonance of the transmission system.

The second method uses state-space equations to estimate the resonance frequency of the transmission system. These equations take into account all the components of the cable and the short circuit impedance of the main grid, with the advantage that is not too more complicated than the first method.

Finally, to validate these two methods, the results obtained via analytic calculus are compared with the results obtained in simulation with PSCAD as described in section 3.2.

3.3.1 State-space equations for the transmission system modeled with a unique "π" circuit

At first, in order to explain with an example the method of the state-space equations, the simplest case is analyzed. The step-up transformer is considered as an equivalent inductance and the main grid as an ideal voltage source with short circuit impedance.

With regards to the submarine cable, this is modeled using several "π" circuits in series, (Khatir et al., 2008). This model has a frequency limit to represent the cable, i.e. the cable model has a valid range in frequency, out of this frequency range the cable model and in consequence the state-space equations cannot be used, since the error becomes too high. For the simplest case, the present case, the cable is modeled as a unique "π" circuit (N=1).

Once the equivalent circuit of the circuit in impedances is determined, it is possible to obtain the frequency response applying the state-space equations, the procedure is as follows:

In the first step, the names and the directions for all the currents of all the branches of the circuit are established as illustrated in, Fig. 12.

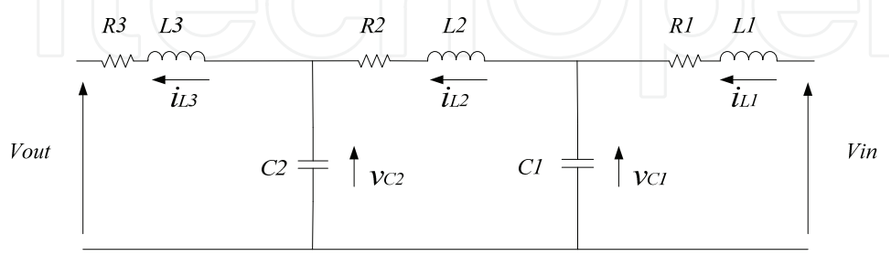

Fig. 12. Mono-phase representation of the transmission system with the submarine cable modeled as a unique "π" circuit

Where: *L1* represents the equivalent inductance of the step-up transformer, *R1* represents the equivalent resistance of the step-up transformer, *R2* represents the resistive part of the

submarine cable, *L2* represents the inductive part of the submarine cable, (*C1*=*C2*) represent the capacitive part of the submarine cable and (*L3* and *R3*) represent *Lsc* and *Rsc* respectively, short circuit impedances.
In the second step, the differential equations are obtained, (12) -(16).

$$\frac{di_{L1}}{dt} = \frac{1}{L1} \cdot \left(Vin - v_{C1} - i_{L1} \cdot R1 \right) \tag{12}$$

$$\frac{dv_{C1}}{dt} = \frac{1}{C1} \cdot \left(i_{L1} - i_{L2} \right) \tag{13}$$

$$\frac{di_{L2}}{dt} = \frac{1}{L2} \cdot \left(v_{C1} - v_{C2} - i_{L2} \cdot R2 \right) \tag{14}$$

$$\frac{dv_{C2}}{dt} = \frac{1}{C2} \cdot \left(i_{L2} - i_{L3} \right) \tag{15}$$

$$\frac{di_{L3}}{dt} = \frac{1}{L3} \cdot \left(v_{C2} - Vout - i_{L3} \cdot R3 \right) \tag{16}$$

Looking at equations (12) - (16), the variables of the differential equations i_{LX} and v_{CX} are independent. In the same way, these variables represent independent physical elements, so, those variables are state variables. Thus, if these equations are written in matrix notation (equation (17)), the state-space matrix is obtained as follows:

$$d/dt \ [x] = [A] \cdot [x] + [B] \tag{17}$$

$$d/dt \cdot \begin{bmatrix} i_{L1} \\ v_{C1} \\ i_{L2} \\ v_{C2} \\ i_{L3} \end{bmatrix} = \begin{bmatrix} -R1/L1 & -1/L1 & 0 & 0 & 0 \\ 1/C1 & 0 & -1/C1 & 0 & 0 \\ 0 & 1/L2 & -R2/L2 & -1/L2 & 0 \\ 0 & 0 & 1/C2 & 0 & -1/C2 \\ 0 & 0 & 0 & 1/L3 & -R3/L3 \end{bmatrix} \cdot \begin{bmatrix} i_{L1} \\ v_{C1} \\ i_{L2} \\ v_{C2} \\ i_{L3} \end{bmatrix} + \begin{bmatrix} 1/L1 & 0 \\ 0 & 0 \\ 0 & 0 \\ 0 & 0 \\ 0 & -1/L3 \end{bmatrix} \cdot \begin{bmatrix} Vin \\ Vout \end{bmatrix} \tag{18}$$

Finally, the poles or eigenvals of the system are calculated (from *A* matrix), to determine its resonance frequency.

3.3.2 State-space equations of the transmission system modeled with N "π" circuits

In the next step forward, the procedure explained in the previous section (3.3.1.), is applied to a generic case where the transmission system has a cable modeled with N "π" circuits, Fig. 13.

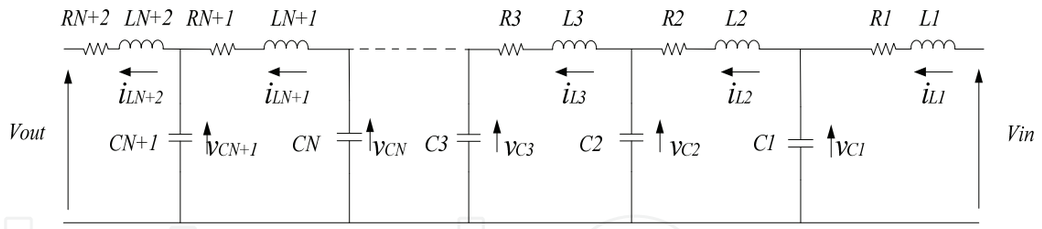

Fig. 13. Mono-phase representation of the transmission system with the submarine cable modeled as N "π" circuits

Where: *L1* represents the equivalent inductance of the step-up transformer, (*R2=R3=RN+1*) represent the resistive part of the submarine cable, (*L2=L3=LN+1*) represent the inductive part of the submarine cable, (*C1* to *CN+1*) represent the capacitive part of the submarine cable and (*LN+2* and *RN+2*) represent *Lsc* and *Rsc* respectively, short circuit impedances.
For the generic transmission system, following the procedure explained in the previous section, the state-space variables are defined and the estate-space equations are obtained. These state-space equations in matrix notation are displayed in equation (19). The reader can find the similarities of the matrix structure in expressions (18) and (19).

$$d/dt\cdot\begin{bmatrix} i_{L1} \\ v_{C1} \\ i_{L2} \\ .... \\ i_{LN+1} \\ v_{CN+1} \\ i_{LN+2} \end{bmatrix} = \begin{bmatrix} -R1/L1 & -1/L1 & 0 & .... & 0 & 0 & 0 \\ 1/C1 & 0 & -1/C1 & .... & 0 & 0 & 0 \\ 0 & 1/L2 & -R2/L2 & .... & 0 & 0 & 0 \\ .... & .... & .... & .... & .... & .... & .... \\ 0 & 0 & 0 & .... & -RN+1/LN+1 & -1/LN+1 & 0 \\ 0 & 0 & 0 & .... & 1/CN+1 & 0 & -1/CN+1 \\ 0 & 0 & 0 & .... & 0 & 1/LN+2 & -RN+2/LN+2 \end{bmatrix} \cdot \begin{bmatrix} i_{L1} \\ v_{C1} \\ i_{L2} \\ .... \\ i_{LN+1} \\ v_{CN+1} \\ i_{LN+2} \end{bmatrix} + \begin{bmatrix} 1/L1 & 0 \\ 0 & 0 \\ 0 & 0 \\ .... & .... \\ 0 & 0 \\ 0 & 0 \\ 0 & -1/LN+2 \end{bmatrix} \cdot \begin{bmatrix} Vin \\ Vout \end{bmatrix} \quad (19)$$

3.3.3 Frequency response of the transmission system via state-space equations

Finally, the frequency response of the transmission system with the submarine cable, the step-up transformer and the main grid of the previous section (Table 1, Table 3 and Table 4) via state-space equations is obtained.
For the submarine cable model, 10 "π" circuits in series are considered. In this way, the cable model is composed by sufficient "π" circuits to make possible the representation of the submarine cable in the correct frequency range, i.e. sufficient to represent correctly the cable until the resonance. In more detail, with 10 "π" circuits it is possible to represent the

submarine cable in a valid range for all the resonances analyzed in the previous section (Khatir et al., 2008), by means of equation (20).

$$f_{\max} = \frac{Nv}{8 \cdot l} = \frac{N}{8 \cdot l \cdot \sqrt{LC}} = 1250Hz \Rightarrow 7884rad / s \tag{20}$$

If the resonance frequency estimated in this way is out of the cable model valid range, it is not valid and the analysis must be repeated with a valid cable model.
Finally, applying the developed generic equation (19), to the considered transmission system, the frequency response depicted in Fig. 14 is obtained.

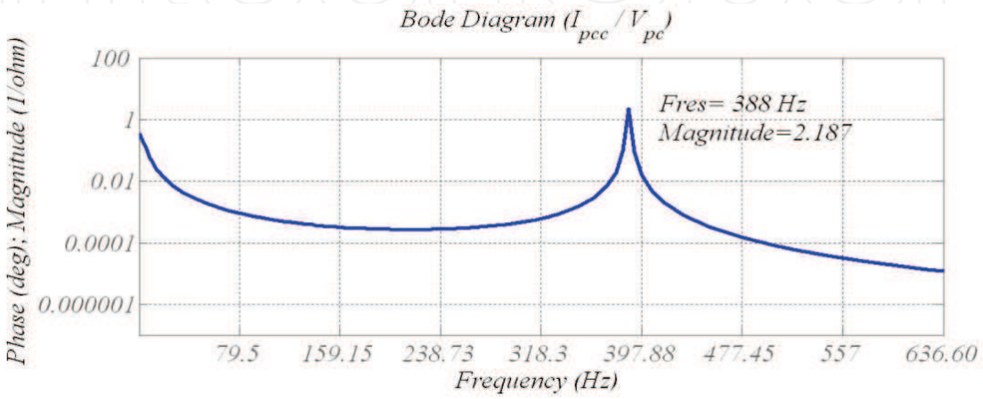

Fig. 14. Frequency response of the transmission system with the cable modeled as 10 "π" circuits in series using state equations

As can be observed in Fig. 14, the first resonance of the system is located at 388 Hz, very close to the 400 Hz estimated via PSCAD simulation. With regards to the amplitude of the resonance, in this case also is an approximation, due to the fact that the calculus is based on a model with lumped parameters, not in a model with distributed parameters which is more accurate.

3.3.4 Frequency response of the transmission system via *RLC* simplification

The other method used to compare with the state-space equations is the simplified *RLC* method, described in (Plotkin et al., 2008). Thus, a comparative is performed comparing the resonance frequency estimated with these three methods for different transmission system. Similarly as done in section 3.2, but in this case, the analysis only varies the cable length and the equivalent inductance of the step-up transformer. The short circuit impedance of the main grid is not taken into account because the simplified *RLC* method does not consider it.
The resonance frequency for the simplified *RLC* method of (Plotkin et al., 2008) is estimated with the following equation (21).

$$f_{\mathrm{Re}sonance} = \frac{1}{2 \cdot \pi \cdot \sqrt{\left(L_{Transfomer} + L_{Cable}\right) \cdot C_{Cable}}} \tag{21}$$

3.3.5 Comparison and validation of the frequency response via analytic calculus

The objective of this section is to validate the state-space equations based method to estimate the first resonance. For that purpose, a comparative of three different methods is carried out.

The method based on PSCAD simulation with the validated cable is considered as the most accurate method.
Hence, Table 5, summarizes the obtained resonance frequencies varying the equivalent inductance of the step-up transformer for the considered three methods. The variation of the equivalent inductance is the same of the section 3.2. (3% to 12%).

Transformers L	3 %	6 %	9 %	12 %
PSCAD simulation	470	400	370	360
State equations	453,6	388,3	356,5	339
Simplified RLC	264,75	218	190,9	171,4

Table 5. Comparative of the resonance frequencies (Hz) obtained varying the equivalent inductance of the step-up transformer

To verify the state-space equations method at different conditions, a second comparative is carried out. In this second case, the cable length is varied, yielding the resonances depicted in Table 6.

Cable length (Km)	*20*	*50*	*80*	*110*
PSCAD simulation	640	400	310	255
State equations	631,8	388,3	297,6	246,6
Simplified RLC	392	218	156,67	124,8

Table 6. Comparative of the resonance frequencies (Hz) obtained varying the cable length

Looking at Table 5 and Table 6, it can be concluded that the state-space equation method is a good approximation for estimating the resonance frequency, even under different transmission conditions options.
On the other hand, the simplified *RLC* method does not provide as accurate results as expected to characterize the resonance frequency. However it could be useful to obtain a very simplified and first approximated value.

4. Frequency response of the offshore wind farm

In the present work, the electric infrastructure of the offshore wind farm's connection is divided into two parts: The transmission system and the inter-turbine grid. The frequency response of the transmission system has been already characterized in previous section, therefore, the next step consist on characterizing the frequency response of the entire electric infrastructure, including the inter-turbine grids. Thus, this second part of the analysis is mainly focused on the inter-turbine grid and its characteristics.
The equivalent impedance of an offshore wind farm varies with changes in the configuration of the inter-turbine grid. As a result, the frequency response of the system varies as well. Consequently, based on the transmission system evaluated in section 3.1, the analysis performed in this section is focused on the effect of different aspects of the wind farm, like: number of feeders (or radials) in the inter-turbine grid or the location of each wind turbine. The analysis is made from the viewpoint of the wind turbine, which is considered the potential harmonic source in normal operation.

Without the appropriate models is not possible to estimate the resonances of the system. In consequence, a scenario is defined in order to base the analysis of the resonances on it.
The considered scenario presents a radial design for the inter-turbine grid, where each one of those radials is composed by 6 wind turbines of 5MW. The voltage level of the inter-turbine grid is medium voltage, 33kV. As regards to the spatial disposition of the wind turbines, there is considered as a rectangle (Hopewell et al., 2006). In short, the simulation scenario has similar features of Nysted, (Fig. 15).

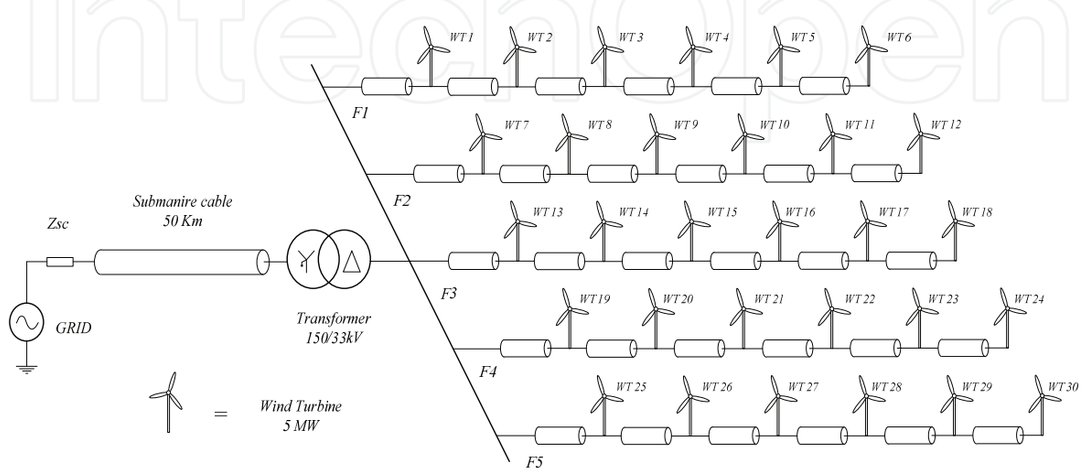

Fig. 15. The lay-out of the offshore wind farm, which is the base of the resonances analysis

Considering that the transmission system is equal to the characterized in section 3.1, the last feature to define the whole offshore wind farm is the inter-turbine submarine cable. Hence, as inter-turbine submarine cable an ABB XLPE cable (Asea Brown Boveri [ABB], 2005) with the adequate nominal voltage and power is chosen. The characteristics of this cable are shown in Table 7.

Parameter	Value
Rated voltage	$30kV$ ($36kV$)
Rated current	765 (65^oC) – 930 (90^oC) A
Cross section of conductor	$800mm^2$
Separation between conductors	$123.65mm$
Buried depth	$1m$
Shields cross section	$35mm^2$
Diameter of conductor	$33.7mm$
Insulation thickness	$8mm$
Diameter upon the insulation	$51.9mm$
Relative dielectric constant	2,30
Resistivity of the conductor d.c. at 20°C	$0,02265Ohm/km$
Resistivity of the conductor a.c.	$0,024959Ohm/km$
Rated capacitance of the cable	$0,38\mu F/km$
Rated inductivity of the cable	$0,31mH/km$

Table 7. Characteristics of the inter-turbine submarine cable (ABB, 2005).

These characteristics are filled into the PSCAD template, for the model explained in section 2 with the corrections exposed in section 2.3.
The aim of this evaluation is to calculate the frequency response of the entire electric connection infrastructure. Thus, the wind turbine model is not considered as a key issue. Therefore, the wind turbines are considered as an ideal controlled voltage source with a *LCL* filter, Table 8. The filter is used to connect the wind turbine to the local inter turbine grid, Fig. 16.

LCL values	*Fres*
0.8 mH-175uF-0.4mH	*550Hz*

Table 8. Characteristics of the LCL filter.

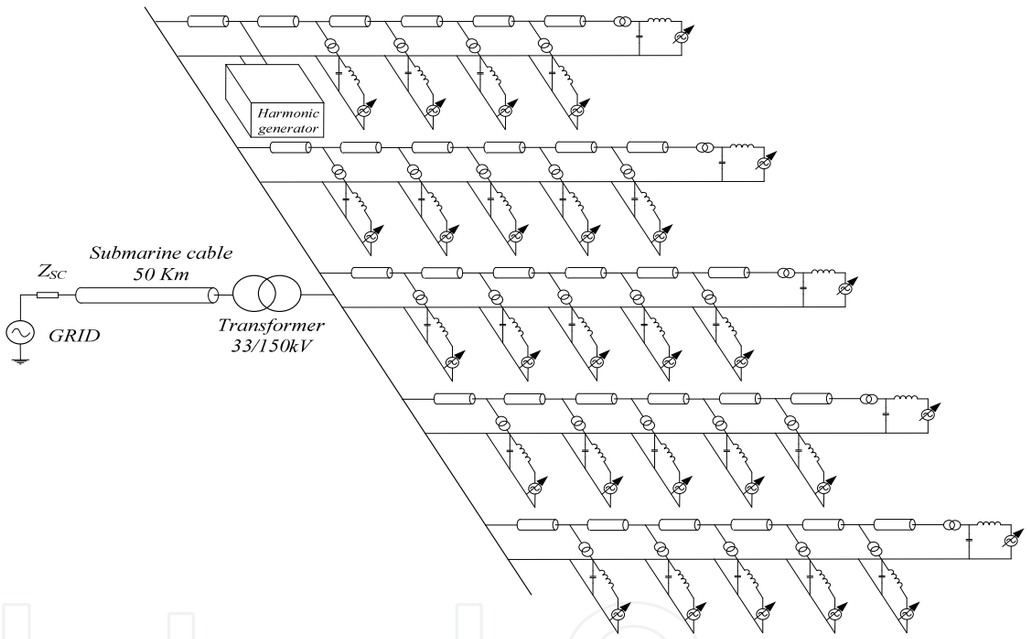

Fig. 16. Simulation scenario of the offshore wind farm, which is the base for the frequency response analysis

Taking the scenario depicted in Fig. 16 as base to estimate the frequency response, the same procedure of section 3.1 is used. In this way, to know the frequency response for a specific wind turbine, it is substituted by a harmonic voltage generator (Fig. 16), which generates a harmonic train in the frequency range of 50Hz-5000Hz, Fig. 6.

4.1 Frequency response of a wind turbine in function of its position in the inter-turbine network

Looking at Fig. 15, it is possible to observe how from the viewpoint of each wind turbine, the equivalent impedance seen is different in function of its location in the inter-turbine grid, i.e. there is not the same equivalent impedance at the output of the 25th wind turbine and at the output of the 30th wind turbine.

To quantify the variation of the frequency responses of each wind turbine, in this section the frequency responses for all the wind turbines of a feeder are estimated. To perform this evaluation, the harmonic voltage source is placed in different positions of the feeder (or radial) and for each position the signals at the PCC are measured. Then, applying the FFT to the signals of the PCC, it is possible to estimate the frequency response for each individual wind turbine.
In the first evaluation, the frequency response of each wind turbine is obtained from the 25th to the 30th. The results for the harmonic currents are depicted in Fig. 17 and the results for harmonic voltages are depicted in Fig. 18.

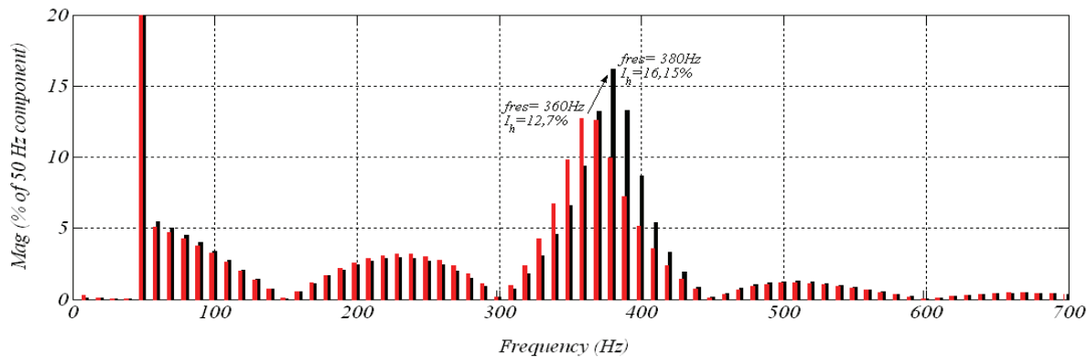

Fig. 17. Harmonic currents at the PCC in function of the location of the harmonic voltage source within the inter turbine grid. For the 30th wind turbine (red) and for the 25th wind turbine (black)

The frequency response of the whole system is similar to the frequency response of the transmission system only. However, the resonance frequency has a short variation. The transmission system presents the resonance at 400 Hz (section 3.1, Fig. 7), but as can be seen from the Fig. 17, the frequency response from the wind turbine viewpoint depends on each wind turbine and is located in the range of 360-380 Hz, close to the 400Hz but not the same.
As seen in section 3.2, the step-up transformer does not allow to transmit 3rd order harmonics and multiples. Looking to the results for the 30th wind turbine, the harmonics located at 360Hz and 370Hz have similar amplitudes in both cases (current and voltage), probably the resonance is between them. This fact, can explain the notorious amplitude reduction.
Applying the FFT to the voltage at PCC (Fig. 18), it is possible to see other two more "small resonances" (attenuated frequencies, but less than the rest), besides the transmission system's resonance.
The first one of these two frequency groups less attenuated than the rest is located between the 1500Hz and 2000Hz. This small resonance has not variations, i.e. is independent to the location of the wind turbine. However, the second group of these frequencies less attenuated is in function of the location of the wind turbine. Thus, in function of the location of the wind turbine, the "small resonance" can be around 2500Hz or 3500Hz. The closer is placed the wind turbine to the offshore substation (shorter cable length to the collector point, and less impedance), bigger is the frequency of the resonance.
Note that these two "small resonances" have significantly smaller amplitude than the main resonance at (360Hz-380Hz).

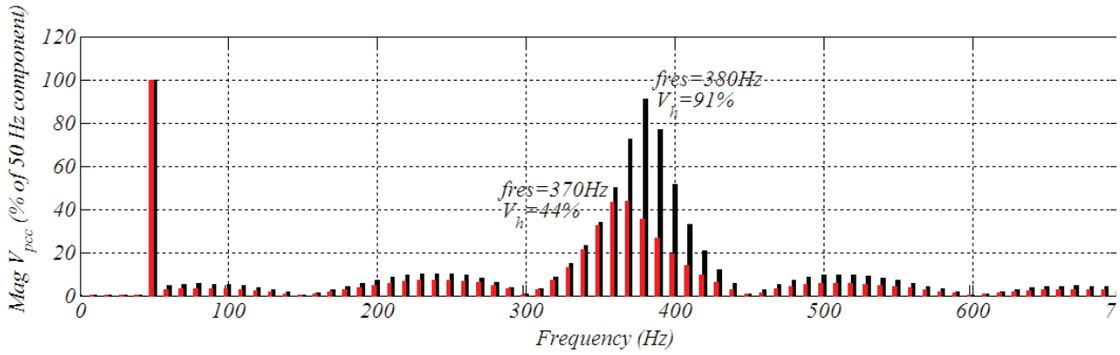

(a)

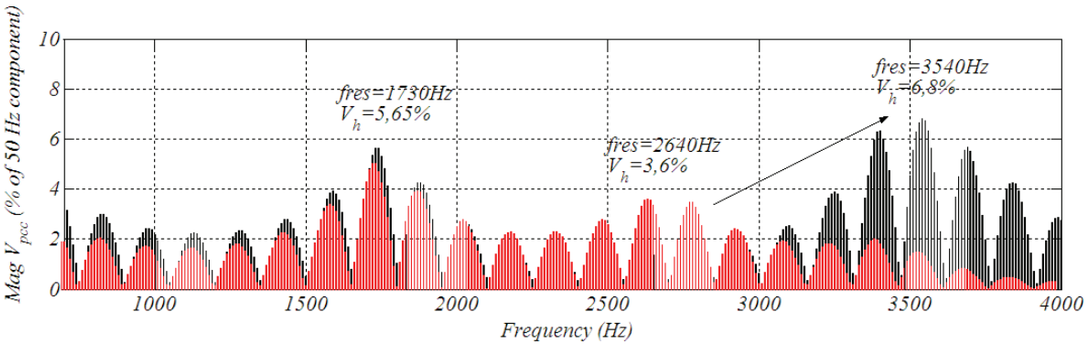

(b)

Fig. 18. Harmonic voltages at the PCC in function of the location of the harmonic voltage source inside the inter turbine grid. For the 25th wind turbine (black) and for the 30th wind turbine (red): (a) more detail in the main resonance and (b) more detail in high frequencies

4.2 Frequency response of the offshore wind farm in function of the feeders in its inter-turbine network

In the first scenario described in section 4, 5 feeders (F1-F5) of 6 wind turbines each one are considered, Fig. 15. However, the internal impedance of the wind farm can have variations with configuration changes, like changes in the number of feeders.

Thus, in this section the frequency response is evaluated for different inter-turbine grid configurations. Inter turbine grids with 2 feeders (F1 and F2) to 5 feeders (F1-F5), Fig. 15 are considered, maintaining the same number of wind turbines for each radial, not the total number of wind turbines of the wind farm.

In this case, the harmonic voltage source is placed at the first wind turbine of each feeder (7, 13, 19 or 25, Fig. 15), because at this point, the second "small resonance" is closer to the fundamental frequency than in any other location of the feeder, Fig. 18 (b). The simulation results (FFT of the current and voltage at the PCC) for the considered configurations are depicted in Fig. 19 and Fig. 20.

From the evaluation of the results of Fig. 19, it is possible to determine that the first and main resonance of the system have not big variations for different configurations of the local inter-turbine grid. However, the second of the "small resonances" (frequency groups less

attenuated) varies with these configuration changes. If there are fewer feeders, the second "small resonance" occurs at higher frequencies.

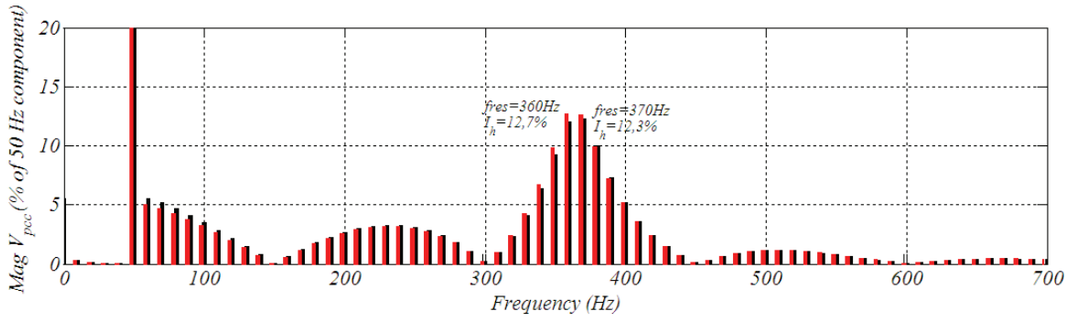

Fig. 19. Harmonic currents at the PCC in function of the number of feeders in the inter-turbine grid: With 2 feeders F1-F2 (black) and with 5 feeders F1-F5 (red)

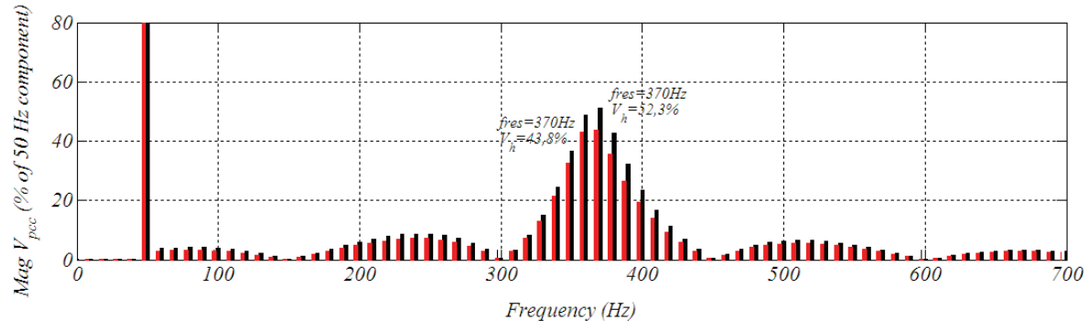

(a)

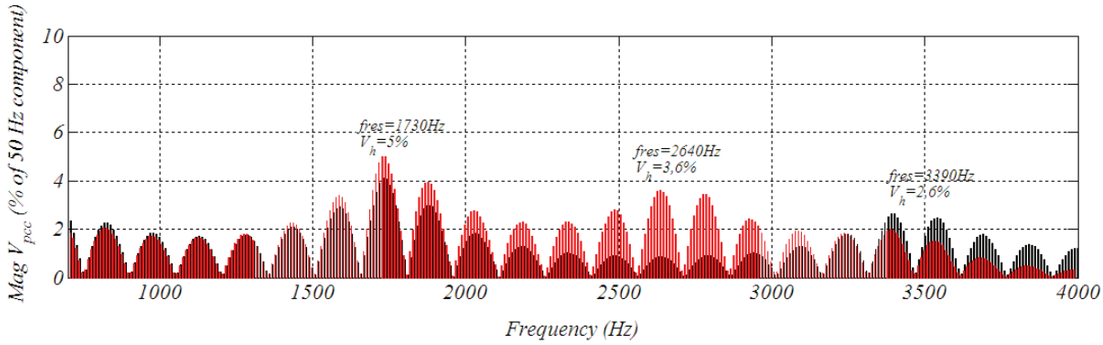

(b)

Fig. 20. Harmonic voltages at the PCC in function of the number of feeders in the inter-turbine grid: With 2 feeders F1-F2 (black) and with 5 feeders F1-F5 (red)

4.3 Frequency response of the offshore wind farm in function of the number of feeders for each step-up transformer's primary

In order to take into account cases where the offshore wind farm have a step-up transformer in the offshore substation with more primary windings than one, the present section

analyzes an inter-turbine network configuration with two primary windings, as depicted in Fig. 21.
The purpose of the analysis is to know how affects this extra primary winding to the frequency response of the offshore wind farm.

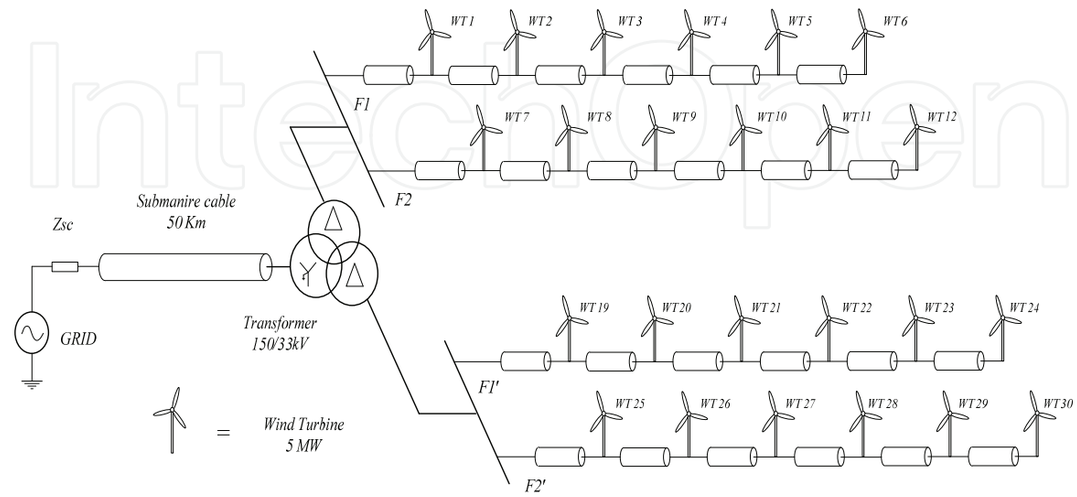

Fig. 21. Simplified scheme of the simulation scenario of the offshore wind farm with two primary windings

To know the influence of the extra winding, the results of the configuration depicted in Fig. 21 and the configuration depicted in Fig. 15 with only two feeders, are compared. The comparison these frequency responses are served Fig. 22 and Fig. 23.

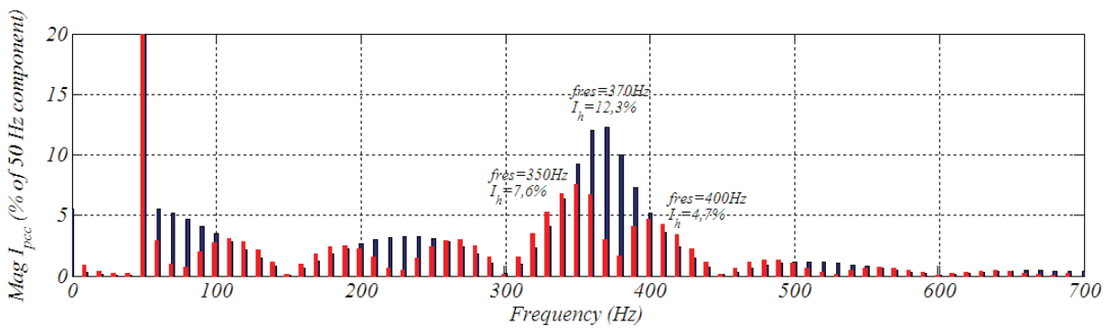

Fig. 22. Harmonic currents at the PCC: With 2 feeders F1-F2 (red) and with 2 feeders on each primary winding F1-F2 and F1′-F2′ (black)

Looking at the results in Fig. 22, it is possible to see that the use of two windings connected as delta-star(grounded)-delta, where the secondary windings have delta connection, does not allow to transmit multiples of 3rd order divided by two harmonics (multiples of 150Hz/2, 75 Hz) to the PCC. As a result, the frequency response of the system from the viewpoint of the wind turbine presents less harmonic components.
However, as can be seen in Fig. 23 (b), for the voltage harmonics, there is a new group of frequencies less attenuated at 2520 Hz.

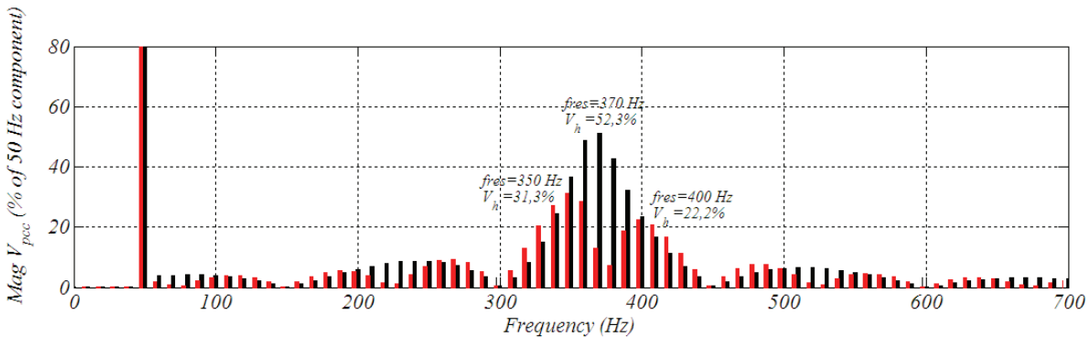

(a)

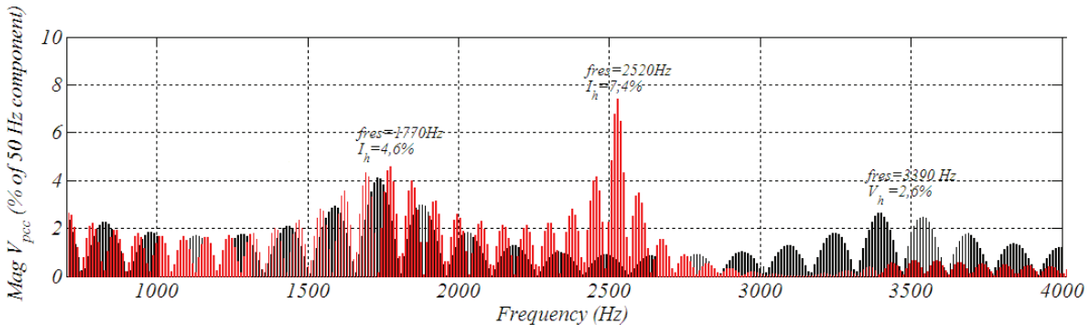

(b)

Fig. 23. Harmonic voltages at the PCC: With 2 feeders F1-F2 (black) and with 2 feeders on each primary winding F1-F2 and F1′-F2′ (red)

5. Conclusions

The study presented in this chapter is focused on the evaluation of the frequency response of the offshore wind farm. This frequency response depends on design parameters such as: the cable length and characteristics, transformers connection and leakage inductance or inter-turbine grid's configuration. The analysis carried out estimates the potential risks on the voltage and current harmonic amplifications.

For that purpose, the state equations are a good approximation in order to estimate in an easy way the frequency response and main resonances of the system. The results obtained with this method are very similar to the simulation results in PSCAD.

As regards to the harmonic risk of the AC offshore wind farms, this kind of wind farms have the potential to amplify low order harmonics due to the iteration between the capacitive component of the submarine cable and the leakage inductance of the step-up transformer. The bigger are the impedances of those two elements, lower is the frequency of the resonance. From the results of this study, it is possible to observe, that the resonance frequency is mainly in function of the characteristics of the submarine cable (its capacitive component).

The main resonance of the AC offshore wind farm from the viewpoint of the wind turbines is the same of the transmission systems resonance. The inter turbine grid, does not cause big variations in the frequency response and for different positions in the inter turbine grid, the

frequency response is similar. However, the inter turbine grid causes "small resonances", which varies with the wind turbines position in the inter-turbine grid. This little resonance has less potential to amplify harmonic components, but, grid codes (like IEEE-519 standard) are more restrictive with the high order harmonics.

To avoid as far as possible the harmonic amplification in normal operation due to the resonance of the transmission system, one good option seems to choose a configuration which the resonance frequency of the transmission system coincides with one of the frequencies that the step up transformer does not allow to transmit, Fig. 9.

6. References

ABB, (2005). XLPE cable systems, user's guide, rev 2.

Breuer, W. & Christl, N. (2006). Grid Access Solutions Interconnecting Large Bulk Power On- / Offshore Wind Park Installations to the Power Grid, *GWREF.*

Castellanos, F., Marti, J.R. & Marcano, F. (1997). Phase-domain multiphase transmission line models, *International Journal of Electrical Power & Energy Systems, Elsevier Science Ltd. vol. 19, No. 4, pp. 241-248.*

Gustavsen, B., Irwin, G., Mangelrod, R., Brandt, D. & Kent, K. (1999). Transmission line models for the simulation of interaction phenomena between parallel AC and DC overhead lines, *IPST 99 Procedings, pp. 61-67.*

Hopewell, P.D., Castro-Sayas, F. & Bailey, D.I. (2006). Optimising the Design of Offshore Wind Farm Collection Networks, *Universities Power Engineering Conference, UPEC '06. Proceedings of the 41st International, 2006, pp. 84-88.*

Jiang, Y.L. (2005), mathematical modelling on RLCG transmission lines, *Nonlinear Analysis Modelling and Control*, Vol. 10, Nº 2, 137-149, Xi'an Jiantong University, China.

Khatir, M., Zidi, S., Hadjeri, S. & Fellah, M.K. (2008). of HVDC line models in PSB/SIMULINK based on steady-state and transients considerations, *Acta Electrotechnica et Informatica Vol. 8, No 2.*

Kocewiak, L.H., Bak, C.L. & Hjerrild, J (2010). Harmonic aspects of offshore wind farms, *Proceedings of the Danish PhD Seminar on Detailed Modelling and Validation of Electrical Componentes and Systems*, Aalborg.

Marcano, F. (1996). Modeling of transmission lines using idempotent decomposition, *M. Sc. Thesis, Department of Electrical Engineering, The University of British Columbia, Vancouver, Canada.*

Meier, S. (2009). System Aspects and Modulation Strategies of an HVDC-based Converter System for Wind Farms, *Ph. D. thesis, KTH Stockholm, ISBN 978–91–7415–292–0.*

Nian, L (2009). *Transients in the collector Grid of a novel Wind Farm topology*, Msc Thesis KTH, Stockholm.

Pigazo, A. (2004). *Método de control de filtros activos de potencia paralelo tolerante a perturbaciones de la tensión de red*, thesis, universidad de Cantabria.

Plotkin, J., Schaefer, U. & Hanitsch, R.E. (2008). Resonance in the AC Connected Offshore Wind Farms, *WECS.*

PSCAD, (2003). User's guide.

Restrepo, L.H., Caicedo, G. & Castro-Aranda, F (2008). Modelos de línea de transmisión para transitorios electromagnéticos en sistemas de potencia, *Revista Energía y computación Vol 16 No 1 p.21-32.*

Sánchez, M.C.M. (2003). *Medida de párametros de ruido de dispositivos activos, basadoa en fuente adaptada*, Thesis, UPC.

Weedy, B.M. & Cory, B.J. (1998). *Electric power systems*, (4th ed.) Wiley, ISBN 0-471-97677-6, Great Britain.

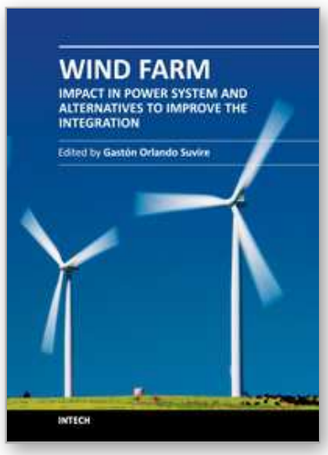

Wind Farm - Impact in Power System and Alternatives to Improve the Integration

Edited by Dr. GastÃ³n Orlando Suvire

ISBN 978-953-307-467-2
Hard cover, 330 pages
Publisher InTech
Published online 28, July, 2011
Published in print edition July, 2011

During the last two decades, increase in electricity demand and environmental concern resulted in fast growth of power production from renewable sources. Wind power is one of the most efficient alternatives. Due to rapid development of wind turbine technology and increasing size of wind farms, wind power plays a significant part in the power production in some countries. However, fundamental differences exist between conventional thermal, hydro, and nuclear generation and wind power, such as different generation systems and the difficulty in controlling the primary movement of a wind turbine, due to the wind and its random fluctuations. These differences are reflected in the specific interaction of wind turbines with the power system. This book addresses a wide variety of issues regarding the integration of wind farms in power systems. The book contains 14 chapters divided into three parts. The first part outlines aspects related to the impact of the wind power generation on the electric system. In the second part, alternatives to mitigate problems of the wind farm integration are presented. Finally, the third part covers issues of modeling and simulation of wind power system.

How to reference

In order to correctly reference this scholarly work, feel free to copy and paste the following:

Markel Zubiaga, Gonzalo Abad, Jon Andoni Barrena, Sergio Aurtenetxea and Ainhoa Cárcar (2011). Evaluation of the Frequency Response of AC Transmission Based Offshore Wind Farms, Wind Farm - Impact in Power System and Alternatives to Improve the Integration, Dr. GastÃ³n Orlando Suvire (Ed.), ISBN: 978-953-307-467-2, InTech, Available from: http://www.intechopen.com/books/wind-farm-impact-in-power-system-and-alternatives-to-improve-the-integration/evaluation-of-the-frequency-response-of-ac-transmission-based-offshore-wind-farms

INTECH
open science | open minds

InTech Europe
University Campus STeP Ri
Slavka Krautzeka 83/A
51000 Rijeka, Croatia
Phone: +385 (51) 770 447
Fax: +385 (51) 686 166
www.intechopen.com

InTech China
Unit 405, Office Block, Hotel Equatorial Shanghai
No.65, Yan An Road (West), Shanghai, 200040, China
中国上海市延安西路65号上海国际贵都大饭店办公楼405单元
Phone: +86-21-62489820
Fax: +86-21-62489821

IntechOpen